







## Article

# Experimental vs. Natural Mineral Precipitation in Modern Microbialites: The Case Study of the Alkaline Bagno Dell'acqua Lake (Pantelleria Island, Italy)

Michela Ingrassia <sup>1,\*</sup>, Aida Maria Conte <sup>1</sup>, Cristina Perinelli <sup>2</sup>, Luca Aldega <sup>2</sup>, Letizia Di Bella <sup>2</sup>,  
Cristina Mazzoni <sup>3,4</sup>, Stefano Fazi <sup>3,4,5</sup>, Francesco Giuseppe Falese <sup>1</sup>, Tania Ruspandini <sup>2</sup>, Agnese Piacentini <sup>3,4</sup>,  
Benedetta Caraba <sup>3</sup>, Andrea Bonfanti <sup>3</sup>, Francesca Gori <sup>2</sup>, Marino Domenico Barberio <sup>6</sup>  
and Francesco Latino Chiocci <sup>1,2</sup>

<sup>1</sup> Institute of Environmental Geology and Geo-Engineering, National Research Council, 00175 Rome, Italy; aidamaria.conte@cnr.it (A.M.C.); francescogiuseppe.falese@cnr.it (F.G.F.); francesco.chiocci@uniroma1.it (F.L.C.)

<sup>2</sup> Department of Earth Sciences, Sapienza University of Rome, 00185 Rome, Italy; cristina.perinelli@uniroma1.it (C.P.); luca.aldega@uniroma1.it (L.A.); letizia.dibella@uniroma1.it (L.D.B.); tania.ruspandini@uniroma1.it (T.R.); francesca.gori@uniroma1.it (F.G.)

<sup>3</sup> Department of Biology and Biotechnology "C. Darwin", Sapienza University of Rome, 00185 Rome, Italy; cristina.mazzoni@uniroma1.it (C.M.); stefano.fazi@cnr.it (S.F.); agnese.piacentini@uniroma1.it (A.P.); benedetta.caraba@uniroma1.it (B.C.); andrea.bonfanti@uniroma1.it (A.B.)

<sup>4</sup> Water Research Institute, National Research Council (IRSA-CNR), Montelibretti, 00015 Rome, Italy

<sup>5</sup> National Biodiversity Future Center (NBFC), Piazza Marina 61, 90133 Palermo, Italy

<sup>6</sup> National Institute of Geophysics and Volcanology (INGV), 00143 Rome, Italy;

marinodomenico.barberio@ingv.it

\* Correspondence: michela.ingrassia@cnr.it



**Citation:** Ingrassia, M.; Conte, A.M.; Perinelli, C.; Aldega, L.; Di Bella, L.; Mazzoni, C.; Fazi, S.; Falese, F.G.; Ruspandini, T.; Piacentini, A.; et al. Experimental vs. Natural Mineral Precipitation in Modern Microbialites: The Case Study of the Alkaline Bagno Dell'acqua Lake (Pantelleria Island, Italy). *Minerals* **2024**, *14*, 1013. <https://doi.org/10.3390/min14101013>

Academic Editor: Javier Sánchez-España

Received: 13 August 2024

Revised: 1 October 2024

Accepted: 1 October 2024

Published: 8 October 2024



**Copyright:** © 2024 by the authors. Licensee MDPI, Basel, Switzerland. This article is an open access article distributed under the terms and conditions of the Creative Commons Attribution (CC BY) license (<https://creativecommons.org/licenses/by/4.0/>).

**Abstract:** Microbial activity has been documented in various lacustrine environments, suggesting its fundamental role in mineral precipitation and, therefore, in the formation of organo-deposits such as microbialites. Many studies are currently focused on documenting how the association of microbes and extracellular polymeric substances (EPSs) may influence the authigenesis of Mg-rich clay minerals and the subsequent carbonate precipitation in growing microbialites in lacustrine environments. In this study, we investigate the present-day microbialites of the alkaline Bagno dell'Acqua lake (Pantelleria Island, Italy) using X-ray diffraction (XRD) scanning electron microscopy (SEM) and energy-dispersive X-ray spectroscopy (EDS). Our results reveal the intimate association of Mg-smectite/carbonate minerals with the EPS and microbes, and, for the first time, we selected microbes belonging to phylum Firmicutes (*Bacillus* sp.), from natural microbialites, to carry out laboratory experiments that testify their direct role in the precipitation of clay and carbonate minerals.

**Keywords:** biomineralization; microbial community; Mg-smectite; organo-sedimentary deposits; alkaline lake

## 1. Introduction

Microbialites are organo-sedimentary deposits formed by microbial communities able to induce the neoformation of authigenic minerals via metabolic pathways [1,2]. Microbialites are present in different aquatic environments such as inland fluvial, lacustrine water, marine coasts and marine extreme environments, and coastal lagoons (e.g., [3–5]) when specific bio-geochemical conditions occur [6]. Microbial organisms have a fundamental role in microbialite formation depending on the complex interplay between environmental and biological factors (e.g., pH, water composition, temperature, salinity, type of microbial community). In lacustrine environments where microbialites are currently growing, processes involving interactions between minerals and microorganisms, such as microbial organisms acting as ideal nucleating agents for mineral precipitation (indirect mineral formation) and

biological control on mineral authigenesis through metabolic processes (direct mineral formation) [7], have captured many researchers' interests.

The chemical composition of the resultant precipitates is strictly influenced by the dominant extracellular polymeric substances (EPSs) produced in microbial mats [8,9], the specific hydrogeochemical conditions, changes in pore water, and the broader fluctuation in water level and chemistry.

It has been widely demonstrated that Cyanobacteria and other microorganisms (e.g., sulfate-reducing bacteria) play an important role in the formation of microbialites [10–12] and in promoting the precipitation of carbonate minerals [9,13–19]. Other studies have focused on bioinduced processes and the role of the microbial extracellular polymeric substance (EPS) on the simultaneous precipitation of Mg-rich clay and carbonate minerals [20–25] and much of the work performed has an experimental character (e.g., [26] for a review, [27]). Ref. [28] proposed a synthesis of laboratory experiments showing the interactions between various bacteria (including *Bacillus* spp.) and clay mineral alterations.

Although microbial mats are commonly associated with the precipitation of carbonate minerals, a few studies have been focused on the role of microorganisms in the precipitation of amorphous phases or Mg-rich clay minerals (such as Mg-smectite and kerolite). However, even though a direct role of microbial activity in the precipitation of these minerals needs to be more deeply investigated, many papers describe the link between microbial mats and Mg-rich clay minerals [29–31]. Due to the coexistence in microbialites of Mg-rich clay and carbonate minerals such as aragonite and hydromagnesite, clay minerals are often considered to promote carbonate precipitation [31,32], an aspect that requires further investigation. In addition, interaction between minerals and microorganisms has also captured many researchers' interests for carbon sequestration purposes (e.g., [33]) and for their industrial applications [26,28,34]. These include the microbial refinement and purification of clay minerals, cleaner synthesis and processing of clay minerals, adsorption, and removal of organic, inorganic, and radioactive pollutants in soils and waters [34].

Modern-growing microbialites associated with Mg-rich clay minerals have been reported in Lake Clifton, Western Australia [22], in the hypersaline lakes on Rottneest Island, western Australia [35], in Great Salt Lake, UT, USA [23], in the Mono Lake, Mono County, CA, USA [20], in different crater lakes in Mexico [36,37], in Lake Alchichica, Puebla, Mexico [38], in Puquios of the Salar de Llamara, northern Chile [31], in Satonda Lake, Indonesia [39,40], in the Van Lake, Turkey [41], in the sabkha of Qatar, Arabian peninsula [42], and in the coastal sabkha of Abu Dhabi, United Arab Emirates [43].

Bagno dell'Acqua is an endorheic alkaline lake (pH ca. 9) located within the Cinque Denti Caldera in the north-eastern sector of Pantelleria Island (central Mediterranean Sea). The lake has a sub-circular shape (0.21 km<sup>2</sup>), and it is about 530 m long and 380 m wide, with a maximum depth of 12 m. The water temperature ranges from 14 °C to 25 °C, reflecting the mixing of meteoric, seawater, and hydrothermal fluids rich in CO<sub>2</sub> and with low amounts of N<sub>2</sub>, O<sub>2</sub>, Ar, CH<sub>4</sub>, H<sub>2</sub>, and He [42,44,45]. The hydrothermal activity is located in the southern sector of the lake with fluids having temperatures ranging from 34 to 58 °C and a pH of about 6.2 [46]. Specifically, the lake water chemistry is characterized by the following general pattern: Na<sup>+</sup> > K<sup>+</sup> > Mg<sup>2+</sup> > Ca<sup>2+</sup> and Cl<sup>-</sup> > HCO<sub>3</sub><sup>3-</sup> > SO<sub>4</sub><sup>2-</sup> > CO<sub>3</sub><sup>2-</sup> for anions expressed in l mmol L<sup>-1</sup> [47,48]. Silica polymorphs such as tridymite, cristobalite, chalcedony, and quartz are at equilibrium, whereas the lake is slightly undersaturated to amorphous silica [48–50]. The bottom lake sediments are mainly characterized by Mg-smectite and aragonite [51] according to previous studies [46,48,52]. Minor amounts of quartz, feldspar, and pyroxene deriving from physical weathering of the surrounding rocks have also been reported [46]. Volcanic rocks exposed on Pantelleria range from rhyolites (pantellerites) to trachytes, and minor transitional basalts, emitted in a wide range of eruptive styles [53]. Along the shores of the lake, rhyolitic and trachytic lavas and domes are exposed [54]. Carbonate and siliceous microbialites have already been reported along the south-western shoreline of the lake [48–50,55]. The carbonate minerals (mainly aragonite with minor amounts of hydromagnesite, calcite, and dolomite) as well

as minor amounts of clay minerals formed within the microbialites have been mainly linked to inorganic processes [48–50]. In this paper, we specifically study the following: (1) the intimate association of Mg-smectite and carbonate minerals with microbes and EPS in the modern microbialites of the Bagno dell’Acqua Lake (Pantelleria Island, Italy), by X-ray diffraction (XRD) and scanning electron microscopy (SEM) coupled with energy-dispersive X-ray spectroscopy (EDS) analyses; (2) we provide, for the first time, the direct role of microbes isolated from microbialites belonging to phylum Firmicutes (*Bacillus* sp.) in promoting the authigenesis of clay and carbonate minerals from natural microbialites by laboratory experiments. Our results provide a better understanding of the natural conditions suitable for the development of Mg-smectite and these findings raised the importance of future research into the wide mechanisms of Mg-clay biomineralization.

## 2. Materials and Methods

### 2.1. Sample Collection and Hydrogeochemical Analyses

Sampling of submerged microbialites was conducted in June 2019, May 2022, and February 2023, mainly in the north-eastern, eastern, and south-western sectors of the lake with a total of 11 sampling sites (Figure 1 and Table S1). In more detail, microbialites from the eastern sector of the Bagno dell’Acqua Lake (C2b and C3b, Figure 1a) have been collected at a depth of 40 cm below the water (Table S1). Microbialites from the north-eastern sector of the lake (C1, C5b and sup, C6, and C8a, bis and bis\_a,) have been generally collected along the shoreline (depth of 0–2 cm) or at a depth of 80 cm. Finally, samples C10, C11, C12a and b, and C13 are from the south-western sector of the lake. Of the latter, only the samples C10, C12a, and b were analyzed (Table 1). Sample C10 is from the volcanic substratum recovered at a depth of 70 cm from the water table whereas samples C12 a and b are from microbialites. During the field campaigns, water electrical conductivity ( $\mu\text{S}/\text{cm}$ ), temperature ( $^{\circ}\text{C}$ ), and pH measurements were performed on-site using the multiparametric WTW Multi 3420 probe with accuracies of  $\pm 0.01$  pH units,  $\pm 1$   $\mu\text{S}/\text{cm}$ , and  $\pm 0.1$   $^{\circ}\text{C}$ , respectively (Table 2). Additionally, two water samples were taken from the center of the lake to analyze major elements, one from the surface and one from a depth of 5 m. Water samples were filtered in situ with a  $0.45$   $\mu\text{m}$  filter and stored into polyethylene bottles. After filtering, samples for the analyses of cations were acidified with HCl. Samples were analyzed by Dionex ICS 5000 and Dionex ICS 1100 chromatographs (manufactured by Thermo Fisher Scientific at Sunnyvale, California, USA) at the Geochemistry Laboratory of the Department of Earth Sciences at Sapienza University of Rome to determine major ions, specifically, anions ( $\text{F}^{-}$ ,  $\text{Cl}^{-}$ ,  $\text{SO}_4^{2-}$ , and  $\text{NO}_3^{-}$ ) and cations ( $\text{Ca}^{2+}$ ,  $\text{Mg}^{2+}$ ,  $\text{Na}^{+}$ , and  $\text{K}^{+}$ ). The carbonate alkalinity ( $\text{HCO}_3^{-}$ ) was measured by titration with  $0.05$  N HCl solution. The cation–anion balance testified the analytical error  $< 5\%$  for each sample. Si was analyzed using an ICP-OES (Thermo Scientific iCap6300 Duo, manufactured by Thermo Fisher Corp. Cambridge, UK, 2012) at the Natural Resources Analytical Laboratory in Alberta (Canada, USA).

**Table 1.** Mineral assemblages of microbialites occurring in Bagno dell’Acqua Lake. Qz—quartz, Cal—calcite, Arg—aragonite, Hmg—hydromagnesite, Sm—smectite, Pl—plagioclase, Kfs—K-feldspar, Mi—mica, Aug—augite, Hl—halite, Py—pyrite. The proportion of minerals expressed in wt %. E—eastern sector; NE—north-eastern sector; SW—south-western sector.

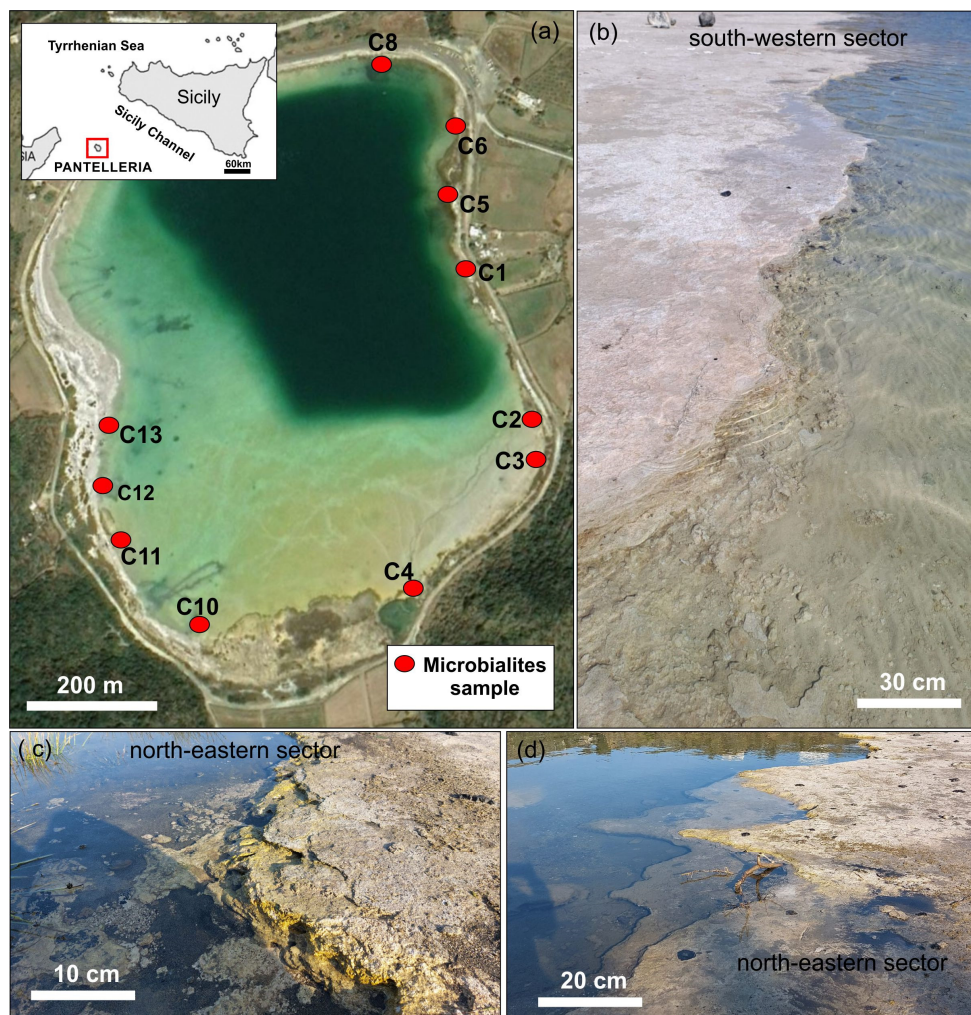
Sample ID	Sector	Depth (cm)	Qz	Cal	Arg	Hmg	Sm	Pl	Kfs	Mi	Aug	Hl	Py
C2b	E	40	2	1	74	-	2	-	21	-	-	-	-
C3b	E	40	2	1	80	13	4	-	tr	-	-	-	-
C1	NE	0	2	1	65	-	3	8	6	-	-	15	-
C5b sup	NE	0	1	-	81	-	5	-	13	-	-	-	-
C5b	NE	0	2	-	17	-	5	5	71	-	-	-	-
C6	NE	2	2	1	78	-	9	-	10	-	-	-	-

Table 1. Cont.

Sample ID	Sector	Depth (cm)	Qz	Cal	Arg	Hmg	Sm	Pl	Kfs	Mi	Aug	Hl	Py
C8 a	NE	0	3	-	19	3	16	-	59	-	-	-	-
C8bis	NE	80	3	-	23	12	12	-	50	-	-	-	-
C8bis a	NE	0	4	1	24	12	6	-	52	-	1	-	-
C10	SW	70	9	-	-	-	-	-	88	-	2	-	1
C12a	SW	0	4	2	67	6	8	12	-	1	-	-	-
C12b	SW	50	2	2	43	-	42	10	-	1	-	-	-

Table 2. Chemical–physical parameters and major ions (both cations and anions) of the water lake.

Date	Temperature (°C)	Electrical Conductivity (mS/cm)	pH	Lat	Long	Ca (mg/L)	Mg (mg/L)	Na (mg/L)	K (mg/L)	Cl (mg/L)	SO <sub>4</sub> (mg/L)	HCO <sub>3</sub> (mg/L)	Si (mg/L)
21 February 2023	14.6	36.5	9.07	36.81692	11.98705	7	186	10,489	462	13,644	1111	3280	11
27 May 2022	24	37.5	9.20	36.81692	77.98705	12	170	9153	502	13,194	1197	3509	9



**Figure 1.** (a) Satellite image of the Bagno dell'Acqua Lake (Pantelleria Island, Italy); (b–d) with a general view of the microbialite sampling locations.

## 2.2. XRD and SEM-EDS

The bulk mineralogical composition of microbialites was determined by X-ray diffraction (XRD) analysis using a Bruker D8 Advance X-ray system equipped with a Lynxeye XE-T silicon-strip detector at the Department of Earth Sciences, Sapienza University of

Rome. Samples were dried in an oven at a temperature of 40 °C overnight. Then, 2 g of microbialite was gently crushed in agate mortar and random-ordered specimens were prepared and run between 2 and 70° 2 $\theta$  with step sizes of 0.02° 2 $\theta$ , 1 s per step (1 h and 6 min long scan), while spinning the sample at 40 kV and 30 mA using CuK $\alpha$  radiation ( $\lambda = 1.5406 \text{ \AA}$ ).

Data were collected with variable slit mode to keep the irradiated area on the sample surface constant and converted to fixed slit mode for semiquantitative analysis. Identification and semiquantitative estimation of mineral phases were performed using the software Diffrac.EVA 5.2 by calculating peak areas and using mineral intensity factors as calibration constants [56].

A qualitative and quantitative approach was used to examine the microbialites by making observations through Scanning Electron Microscope SEM-EDS, FEI Quanta 400, at the SEM Laboratory of the Earth Science Department, Sapienza University of Rome (Italy), in order to describe their morphological, compositional, and biological characteristics.

The microbialite samples were collected and immediately stored in specific jars in order to avoid any contamination. Whole sediments were attached to 12.5 mm SEM stubs using carbon tabs.

The samples were then coated in gold using an Emitech K550X sputter coater, with a routine cycle time for coating SEM samples with conductive coating (5–15 nm) of gold (Au) typically lower than four minutes.

SEM micrographs and EDS spectra were obtained by using a standardized method, with an accelerating voltage ranging between 15 and 20 kV in high vacuum mode; hence, the focus was adjusted to match the change in working distance (~11 mm) over the same range of the specimen and an improved image was obtained, ranging between 5 and 100  $\mu\text{m}$  resolution.

SEM-EDS was employed to obtain chemical analysis and microtextural information on fragments representative of all the microbialites, as well as a careful characterization of biological evidence.

### 2.3. Bacterial Isolation and Identification

For mineralization experiments, bacterial cells of 3bis8 strain grown at saturation in LB liquid media (1% tryptone, 0.5% yeast extract, 1% NaCl) were deposited onto solid B4HLU media consisting of B4 media [57], using lake water filtered through a 0.22  $\mu\text{m}$  membrane (the lake water accounted for roughly 70% (v/v) of the total volume), and supplemented with 0.4% yeast extract, 0.5% dextrose, and 0.3% urea. To this mixture, 5% autoclaved Bacto agar was added, resulting in a final agar concentration of 1.5% [58]. Plates were incubated at 28 °C for 34 days; then, samples were put on a stub and analyzed through SEM and EDS. Uninoculated culture media were used as controls for the experiments, and an experiment was also conducted under the same conditions with the control bacterium *Escherichia coli* DH5 $\alpha$ .

Culturable bacteria were isolated from a fragment of crushed submerged microbialites from the site C3 (see Figure 1) diluted 10<sup>-3</sup>, spread onto Bagno dell'Acqua Lake pH9 plates and incubated at 28 °C for four days [58]. One of these, named 3bis8, was used in this study. Characterization at molecular levels was performed as described by [59,60]. The analysis of the resulting sequences with the online BLAST program [https://blast.ncbi.nlm.nih.gov/Blast.cgi?PRoGRAM=blastn&PAGE\\_TYPE=BlastSearch&LINK\\_LOC=blasthome](https://blast.ncbi.nlm.nih.gov/Blast.cgi?PRoGRAM=blastn&PAGE_TYPE=BlastSearch&LINK_LOC=blasthome) (accessed on 6 November 2023) revealed that the closest bacterial relative to the 3bis8 strain was *Bacillus* sp. (98% identity to *Bacillus cereus*). Sequence was deposited to Genbank NCBI with the accession number OR772953.

Additional fragments of crushed submerged microbialites, from the site C3, were fixed in ethanol (50% final concentration) immediately after collection, and stored frozen at -20 °C until further analysis. To visualize Bacilli within the original microbialite fragments, the CARD-FISH technique was employed [61,62]. A horseradish peroxidase-labeled oligonucleotide probe targeting specific rRNA (LGC354a, Biomers, Ulm, Germany) was

used to detect various genera of Bacilli (phylum Firmicutes), including *Bacillus*, *Exiguobacterium*, *Leuconostoc*, *Weissella*, and *Lactobacillus* [63,64]. DAPI staining was applied to the cells for visualization. The stained microbialite samples were then observed using a confocal laser scanning microscope (CSLM; Olympus FV1000). DAPI-stained cells were excited by 405 nm light, emitting in the 430–470 nm range (blue fluorescence), while hybridized bacterial cells were excited by a 488 nm Ar laser and viewed in the green channel (500–530 nm emission). Mineral crystals were detected by their reflection signal at 405 nm from a diode laser, appearing gray [65]. A 3D reconstruction of the CSLM images was created using IMARIS 7.6 software (Bitplane, Switzerland).

### 3. Results

#### 3.1. Microbialite Fabric

As already reported, the peculiar environmental conditions of the alkaline Bagno dell'Acqua Lake favor the deposition of both carbonate and siliceous microbialites [49,50]. The organo-deposits grow in shallow waters close to the shoreline mainly in the north-eastern and south-western sectors of the lake and show different macroscopic fabrics. In the south-western sector, the microbialites form a uniform white platform that sometimes is emerged and subjected to desiccation (Figure 1b). Generally, these microbialites show a vertical layering that from top to bottom is composed of a 1 mm thick light brown layer overlying a millimetric-thick well-defined green layer and centimetric-thick white layer (Figure 2a–c). In the eastern sector of the lake, the microbial mats show a terraced accretion, mostly lithified with a brownish layer (Figure 1c,d). Sometimes, the deepest part of the lithifying microbial mat is characterized by a black layer up to 1 mm thick (Figure 2a). The microbialites appear roughly laminated and vary from soft to partly consolidated.

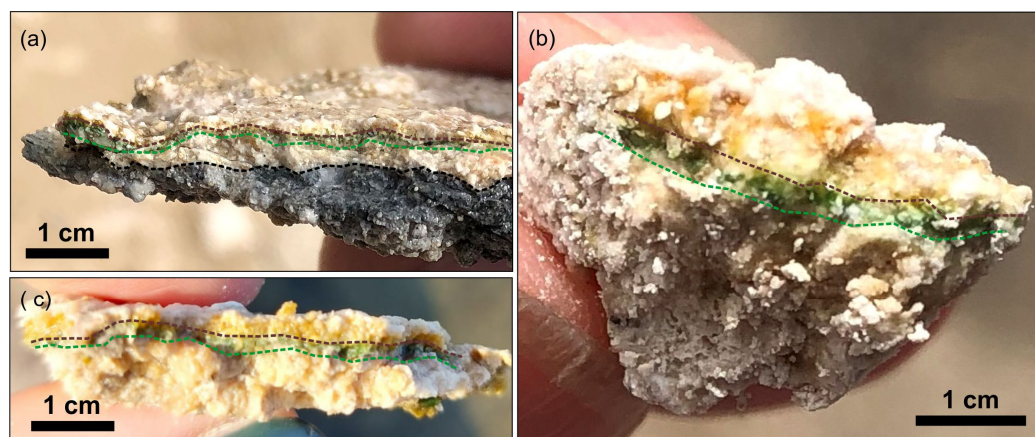


**Figure 2.** (a–c) Photographs of distinct Bagno dell'Acqua microbialites (samples C1, C2, and C13) showing their vertical layering: uppermost light brown layer, a well-defined green layer, a thick white layer, and sometimes a black layer (dotted lines indicates the main layers analyzed in this study).

#### 3.2. X-ray Diffraction of Microbialites

Microbialites from the eastern sector of the Bagno dell'Acqua Lake C2b and C3b have a mineral assemblage (Table 1) mostly made up of carbonate minerals such as aragonite, hydromagnesite, and calcite that account for 75% to 94% of the overall composition and small amounts of smectite (2–4%) and quartz (2%).

Sample C2b contains K-feldspar grains from the volcanic substratum. Most of the samples of microbialites from the north-eastern sector of the lake (C1, C5b and sup, C6, and C8a, bis and bis\_a,) are thin layers of microbial mats and carbonate minerals atop the volcanic substratum; therefore, the inorganic fraction of the microbialites is a mixture of primary volcanic minerals and carbonate mud precipitated in situ with the mediation of microbes. When the primary volcanic minerals prevail (e.g., sample C5b), their content can be up to 76% including K-feldspar, clinopyroxene, and plagioclase while the carbonate mud

of the microbialites (e.g., C5b sup) is generally composed of aragonite (from 19% to 81%), hydromagnesite (up to 12%), and subordinate amounts of calcite (1%). Smectite occurs in all the samples with contents ranging from 3% to 16% and quartz does not exceed 4%. Occasionally, halite crystals precipitate as in the case of sample C1 (Table 1). Among the samples from the south-western sector of the lake, the C10 from the volcanic substratum is mostly made of K-feldspar (88%), quartz (9%), and subordinate amounts of augite (2%) and pyrite (1%). C12 microbialites are mostly composed of aragonite (43 to 67%), calcite (2%), hydromagnesite (up to 6%), smectite (from 8 to 42%), and of detrital grains from the volcanic substratum such as plagioclase, quartz, and mica (Figure 3).

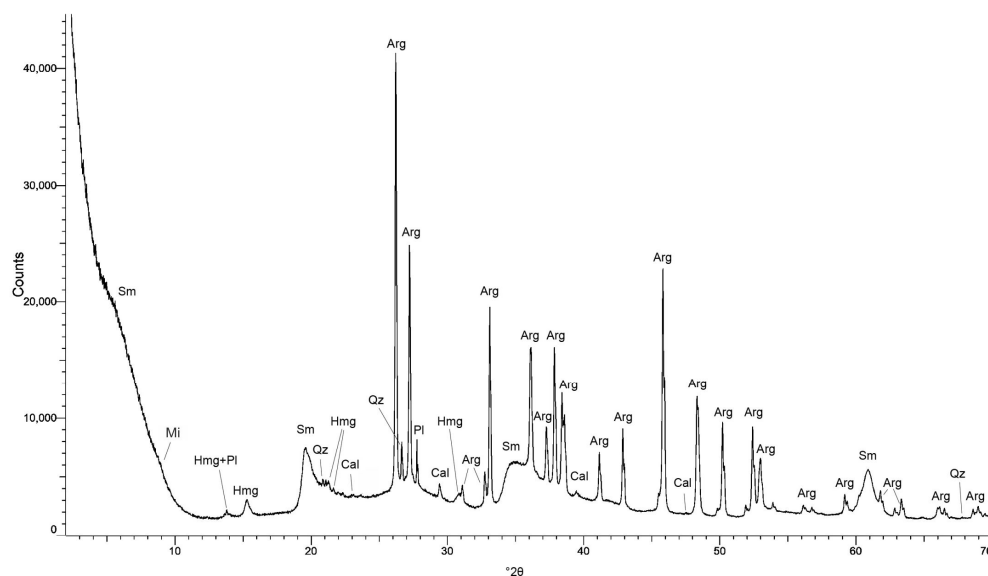


**Figure 3.** Selected X-ray diffraction pattern for the microbialites occurring in the south-western sector of the lake (sample C12). Qz—quartz, Cal—calcite, Arg—aragonite, Hmg—hydromagnesite, Sm—smectite, Pl—plagioclase, Mi—mica.

### 3.3. SEM-EDS Analyses of Microbialites

For the aim of our study, we focused the scanning electron microscope analyses mostly on the characterization of the neoformed silicate phase and the associated carbonates found together with microbes and diatoms, close or trapped into the extracellular polymeric substance (EPS; Figure 4). In this respect, SEM-EDS observations highlighted a substantial amount of a silicate phase, likely corresponding to the smectite identified by XRD. A peculiar compositional character of such a silicate phase is that it is mostly composed of Si and Mg, with a very low amount of Al). This led to suggestions that it may represent a type of Mg-rich smectite (such as stevensite, saponite). For this reason, hereon, we use the “general” term Mg-smectite to indicate the silica phases observed within the microbialites.

In detail, in the south-eastern sector of the lake, the samples (C1, C2, and C3) are characterized by Mg-smectite, halite, and carbonate minerals. Occurrence of no well-preserved pennate diatoms is also observed. Sample C4 is in the correspondence of the thermal spring, where the chemical conditions of the lake water (pH 6.44, 53.9 °C, and conductivity of 70.9  $\mu\text{S}/\text{cm}$ ) are different than the rest of the lake. In this sample, the main phases are represented by quartz and carbonate minerals. Centric and pennate diatoms are observed too (Figure S1a,b). In the north-eastern sector of the lake, the samples (C5 and C6) are characterized by Mg-smectite, carbonate, quartz, and particles showing the presence of the extracellular polymeric substance (EPS; Figure 4). The presence of Cl in some EDS spectra suggests the occurrence of halite, e.g., Figure 4h. Pennate diatoms are also present.

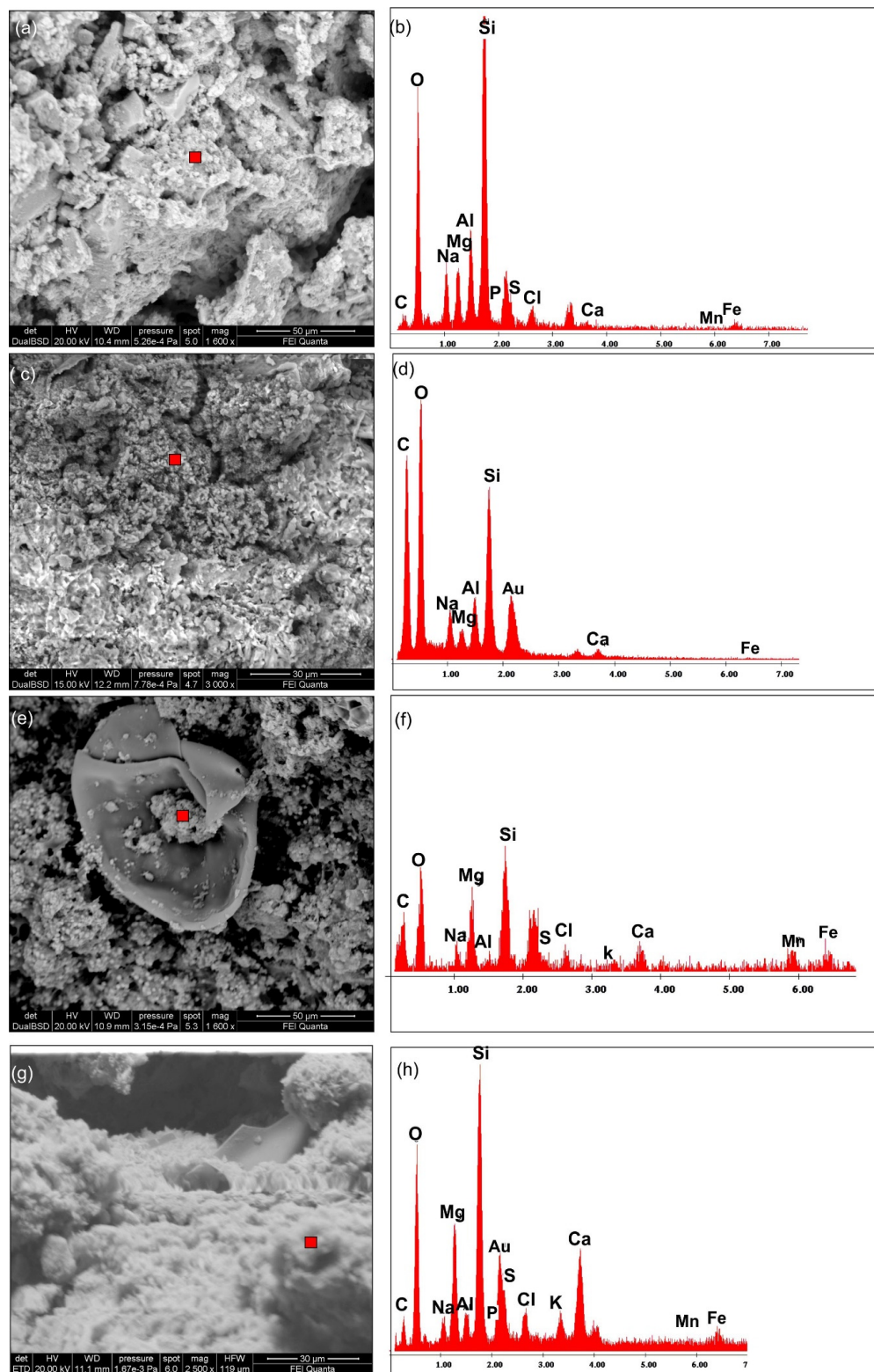


**Figure 4.** (a,c,e,g) SEM images and (b,d,f,h) relative EDS spectra showing the multi-elemental compositions of selected microbialites (i.e., C1, C5, C8, C12) ranging from Mg-smectite to extracellular polymeric substance (EPS). The location of EDS analyses is indicated by red square on the SEM images.



In the northern sector, sample C8 is characterized by Mg-smectite, hydromagnesite, halite, and, as in samples C5 and C6, particles with the EPS. Occurrence of well-preserved pennate diatoms is also observed. Hydromagnesite is observed as both rosette-like formation (Figure 5a) and spheres (Figure 5b), with diameters varying from 50 to 150  $\mu\text{m}$ .

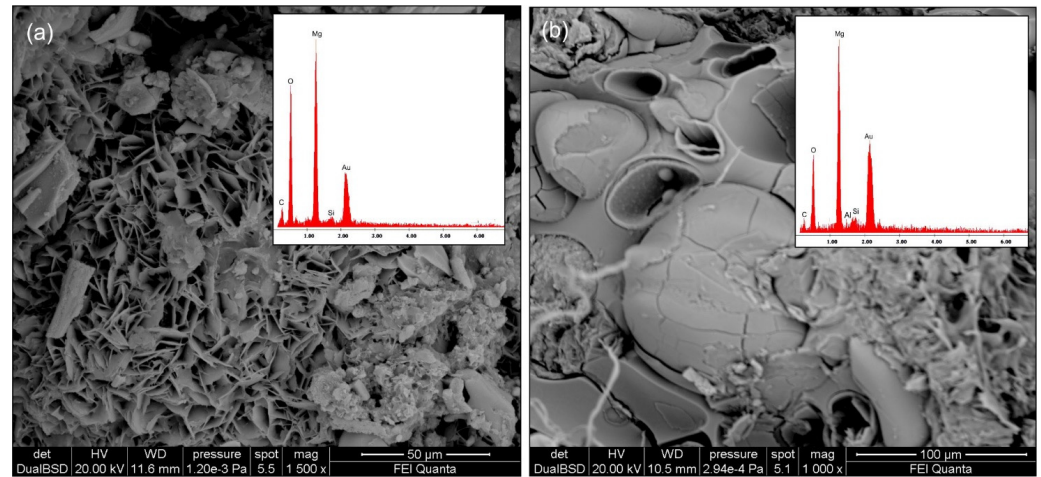


**Figure 5.** SEM images with relative energy-dispersive X-ray spectra (EDS) showing presence of hydromagnesite as (a) rosette-like formation and (b) spheres (C8 a and C8bis).

In the south-western sector of the lake, the samples (C10, C11, C12, and C13) are characterized by the presence of Mg-smectite, Ca-carbonate, halite, and alkali feldspar. Occurrence of well-preserved pennate and reworked diatoms are also observed. The Mg-smectite, characterizing all the analyzed samples, appears as sub-spherical aggregates with a smooth outer layer with a size of a few microns (Figure 6a,b).

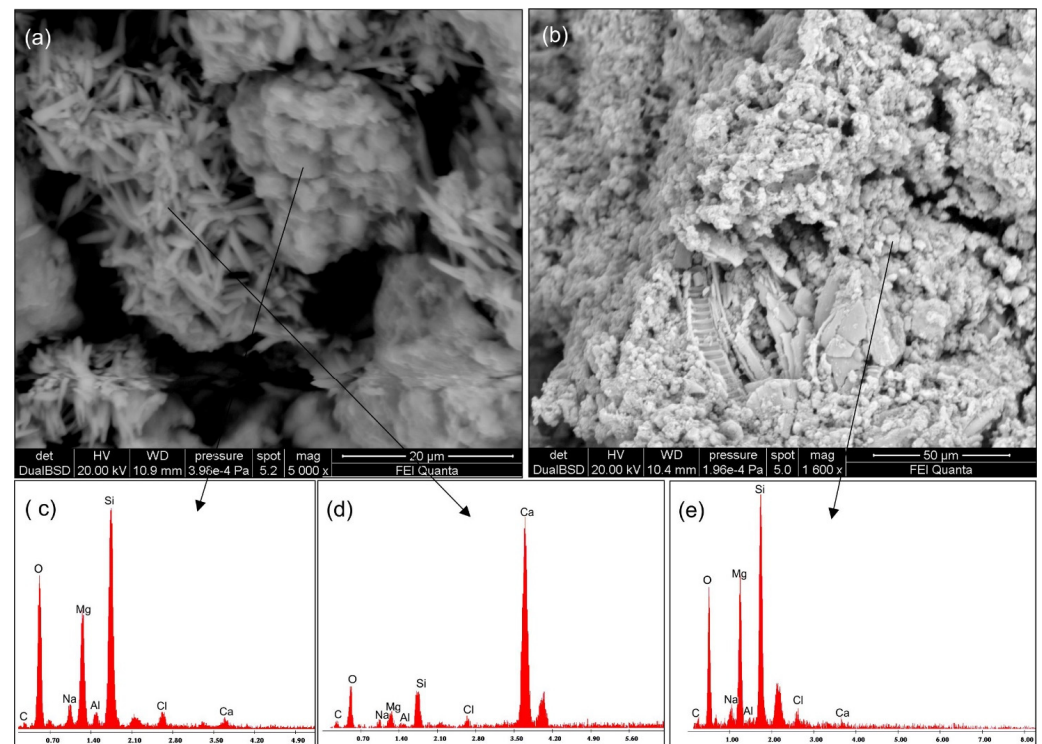


**Figure 6.** (a,b) Scanning electron microscopy (SEM) images and (c–e) energy-dispersive X-ray spectra (EDS) of the main phases (Mg-smectite and carbonate minerals) characterizing the Bagno dell'Acqua microbialites (C12 sample).

Mg-smectite is sometimes associated with white acicular crystals of Ca-carbonate ranging in size from a few  $\mu\text{m}$  to 20  $\mu\text{m}$ , which probably refer to aragonite based on the crystal habit and its weight percent quantified by XRD (Figures 6a and 7a). These crystals are often associated with the EPS (Figure 7b,d), locally with populations of filamentous (Figure 7c) and coccoids bacteria with diameters of about 5  $\mu\text{m}$  that appear encased in the EPS (Figure 7d). In addition, visible signs of the dissolution and degradation of diatom frustules are observed (Figure 7e,f).

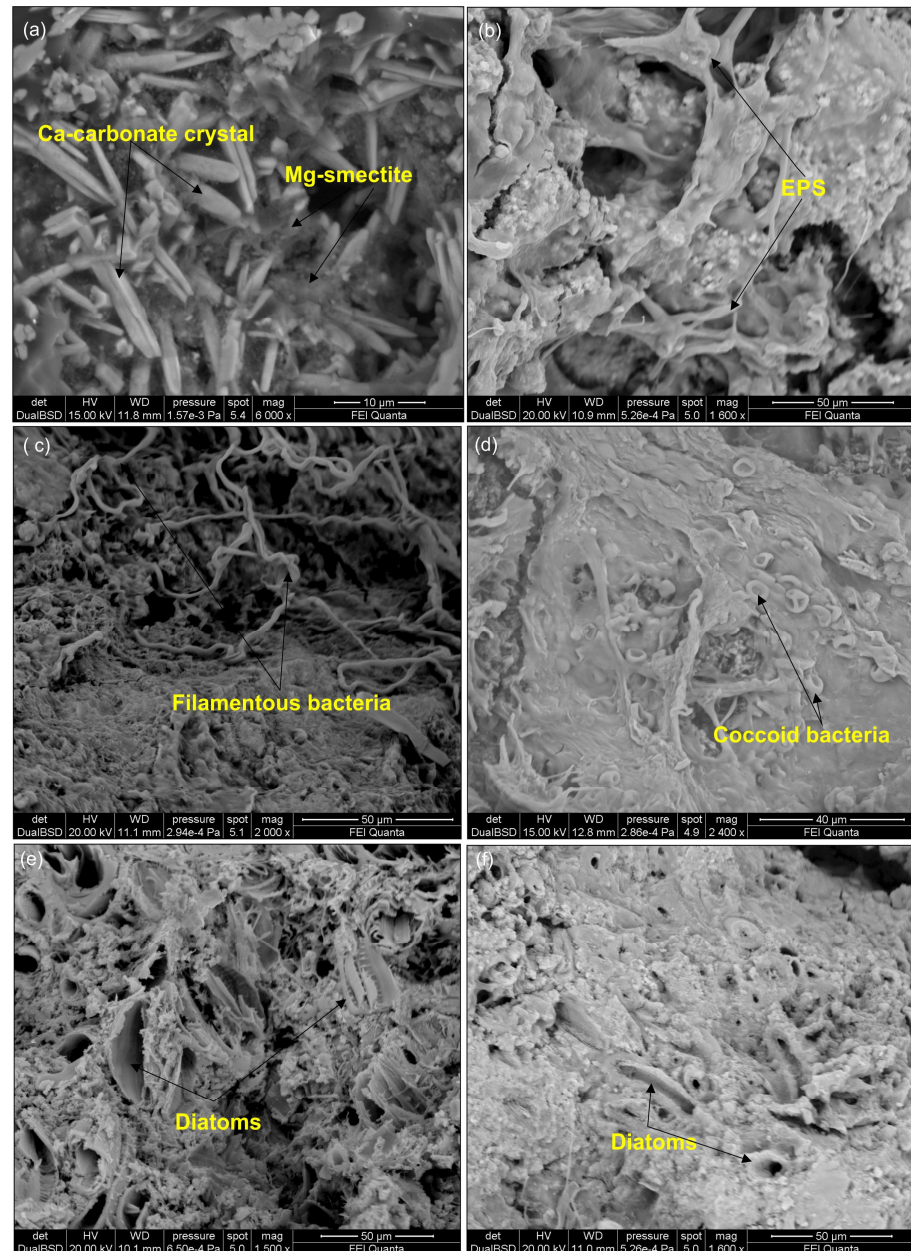


**Figure 7.** Scanning electron microscopy (SEM) images showing the main microstructures characterizing the Bagno dell'Acqua microbialites. (a) Mg-smectite with acicular crystal of carbonate minerals (sample C1); (b) evidence of extracellular polymeric substance (EPS; sample C10); (c) populations of filamentous bacteria (sample C12a); (d) coccoids bacteria encased in EPS (sample C13); (e,f) diatoms with visible signs of dissolution and degradation (samples C1 and C2).

### 3.4. Laboratory Experiments

To investigate the role of bacteria in mineral formation, we analyzed the biomineralization capability of microbes belonging to phylum Firmicutes (*Bacillus* sp.). It should be noted that, by applying the CARD-FISH technique, we were able to visualize and show the spatial distribution of the class Bacilli and other prokaryotes within the intact layers of the natural microbialites, from the same site from where the *Bacillus* sp. was isolated, confirming a possible direct role of these microorganisms on microbialite formation in the natural environment (Figure 8).

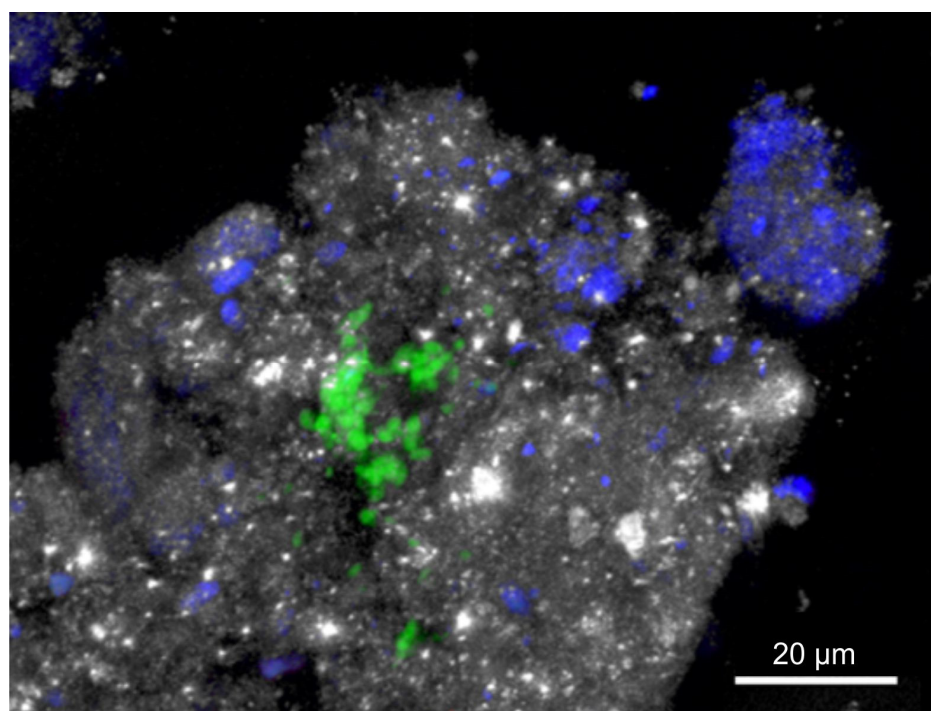


**Figure 8.** CLSM images illustrate the spatial arrangement of bacteria from the Bacilli class (Firmicutes phylum) in green, along with other prokaryotes in blue, as identified by CARD-FISH in the surface layers of the natural microbialite at site C3. Bacterial cells were excited using a 488 nm Ar laser and detected in the green channel (500–530 nm emission range). Mineral crystals were visualized through their reflection signal at 405 nm using a diode laser, appearing gray in the images. Scale bar = 20  $\mu\text{m}$ .

The SEM images in Figure 9 indicate that products of the strain are some isolated fragments with a size in the order of a few microns. The most important feature of these fragments is that they, or part of them, have a shape resembling the mineral phases observed in the natural microbialites. In particular, the pale-grey grains shown in Figure 9a (indicated by green arrows) and Figure 9e display a morphology close to that of clay minerals or mineral precursor phases [66]. In Figure 9c, halite is also detected, as shown by the EDS spectrum. EDS analyses confirm this indication as the spectra reported in Figure 9b,d,f likely represent, respectively, compositions close to those of Mg-smectite. In more detail, in the spectrum of Figure 9h, halite is also detected as testified by the presence of Na and Cl peaks. In the analyzed fragments shown in Figure 9g, some additional features are evident such as traces of EPS fibers (white arrow) and the presence of bacterial cells (Figure 9e,i, yellow arrows). The relative EDS spectrum (Figure 9h) is characterized by a different Si-Al ratio than the previous ones, a higher Fe concentration, presence of K, and significantly high carbon concentration likely due to the presence of both EPS and bacteria.

It is worthy noting that, differently from the previous compositions, the white grains present in Figure 9m display a clear calcium-carbonate composition (Figure 9n).

In summary, the aggregates precipitated by 3bis8 *Bacillus* sp. in laboratory experiments by using the Bagno dell'Acqua water lake, display shapes and compositions ranging from

Mg-smectite to EPS compositions up to Ca-carbonate. This assemblage is very similar to what has been observed in the natural microbialites (i.e., samples C1, C5, C6, C8, and C12).

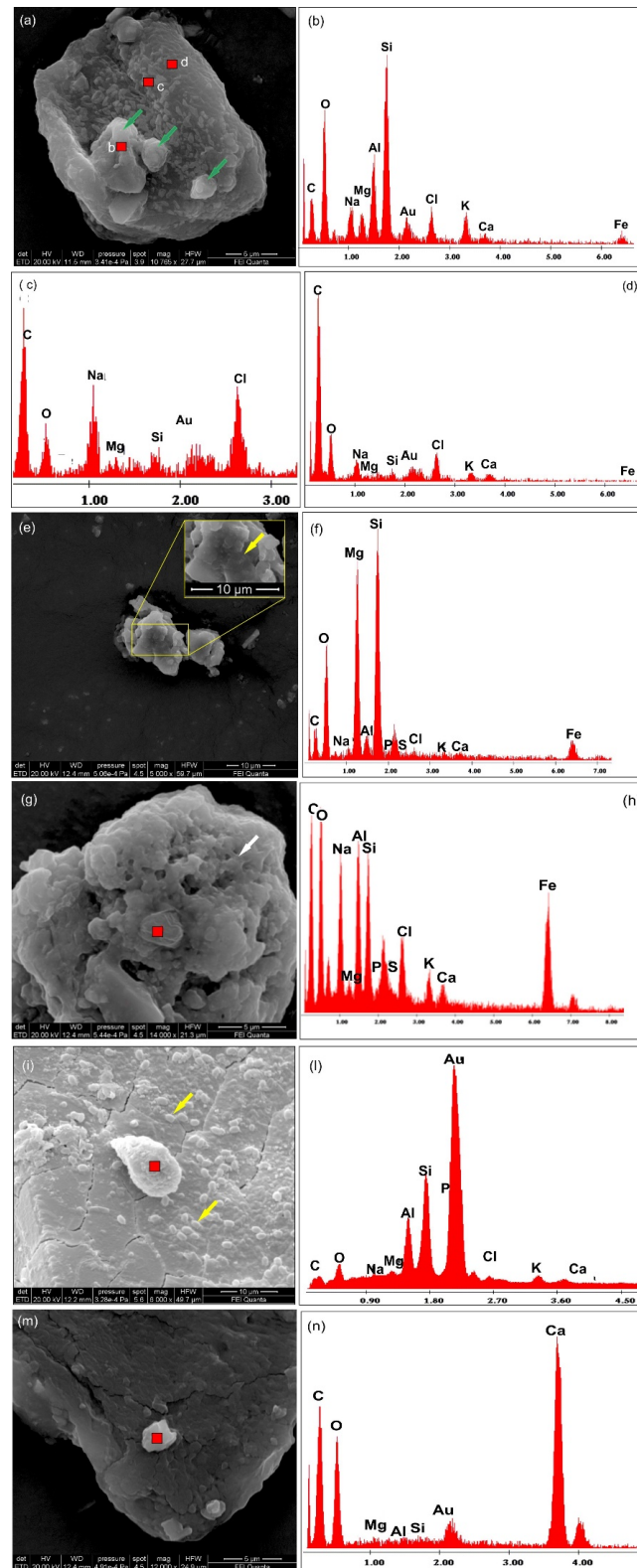


**Figure 9.** (a,e,g,i,m) Scanning electron microscopy (SEM) images and (b–d,f,h,l,n) energy-dispersive spectra (EDS) of the clay/clay precursor phase and carbonate aggregates precipitated with 3bis8 *Bacillus* sp. in laboratory experiment using the Bagno dell’Acqua water lake. Yellow arrows indicate bacterial cells; white arrow indicates EPS fibers.

Finally, in the SEM-EDS analyses performed on the negative control experiment (i.e., without bacteria), no silicate compounds were observed, but only halite precipitation occurred (Figure S3), while in the experiment carried out using the control bacterium *E. coli*, in addition to halite, the presence of sporadic multi-elemental (Ca, Si, Mg, Al) particles lacking a defined morphology was observed (Figure S4).

### 3.5. Water Chemistry

In Table 2, we report the chemical–physical parameters and geochemical results of the water lake samples. The concentration of major elements expressed in mg/l showed the general pattern, as also recognized in a previous study [49],  $\text{Na}^+ \gg \text{K}^+ \gg \text{Mg}^{2+} \gg \text{Ca}^{2+}$  for cations and  $\text{Cl}^- \gg \text{HCO}_3^- \gg \text{SO}_4^{2-}$  for anions.

We also calculated the saturation indices of the aqueous solutions using the PHREEQC Interactive software (Version 3.7.3) [67], and the results are shown in Figure 10. The analyzed solutions turn out to be supersaturated with respect to calcite, aragonite, dolomite, chrysotile, huntite, magnesite, and sepiolite.

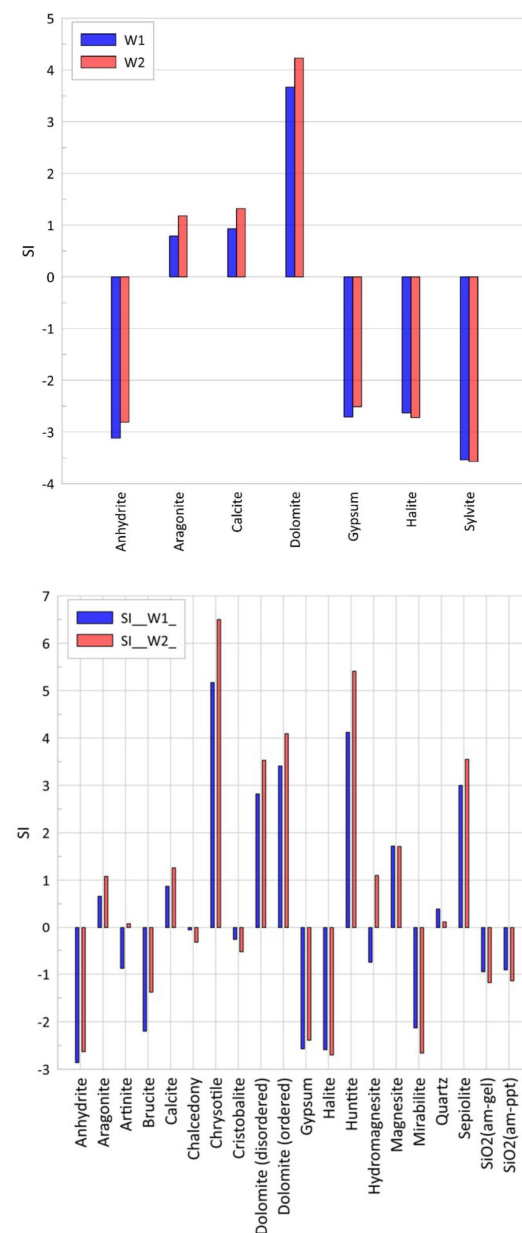


**Figure 10.** Saturation indices (SI) of the two water lake samples (i.e., W1 and W2) are shown with blue and red bars.

#### 4. Discussion

Laboratory experiments pointed out, for the first time, the role of microbes belonging to phylum Firmicutes (*Bacillus* sp.) in promoting the precipitation of clay minerals, including Mg-smectite, and carbonate minerals in the presence of filtered lake water. The XRD results of the lithifying microbial mats of the Bagno dell'Acqua Lake revealed that Mg-smectite occurs in all samples with contents varying from 16% to 42% together with significant amounts of carbonate minerals (aragonite, hydromagnesite, and calcite). The SEM-EDS investigations confirm the intimate association of Mg-smectite/carbonate minerals with microbes and extracellular polymeric substances (EPSs).

##### *Biogenic Origin of the Mg-Clay Minerals Forming the Bagno Dell'acqua Microbialites*

Mg-smectite and carbonate minerals are relatively common components in modern and ancient lake systems, especially in volcanic areas. In these contexts, lake water chemistry, which is influenced by the lithology of the surrounding catchment, controls carbonate and silicate production [68]. The surrounding Pantelleria soils are characterized by the presence of alkali feldspar, clinopyroxene, olivine, quartz, and Fe-Ti oxides as the main mineralogical phases, with a variable content of clay minerals such as kaolinite, illite, and smectite [69]. Therefore, the presence of clay minerals in sediments and deposits developed on the lake are partly linked to weathering and water-rock interaction processes [48]. Silica activity is usually high in alkaline lake waters and together with dissolved magnesium may lead to the formation of significant amounts of authigenic clay minerals by direct precipitation, or by the transformation of precursor materials such as glassy pyroclastics and/or detrital clays [70–72]. In addition, the type and composition of the silicates depend on the silica and Mg sources, which can be influenced by the presence of microorganisms (e.g., [73]). Regarding the carbonate phases, hydrogeochemical results (Table 2 and Figure 10) suggest the composition of the system is predominantly influenced by groundwater and evaporation processes [45,46]. The prevalence of Na and Cl ions is a typical feature of groundwater on Pantelleria Island, resulting from the mixing of groundwater with seawater [45]. Additionally, the leaching of volcanic rocks surrounding the lake and water-rock interaction processes contribute to the enrichment of alkaline elements [74].

Considering these statements, this study aims to better understand the processes leading to the authigenesis of Mg-clay minerals, highlighting the importance of the microbial role, in the microbialites growing in the Bagno dell'Acqua Lake.

The mineral sequence leading to the lithification of the analyzed microbialites is herein proposed. In the initial phase, the microbial community, mainly composed of phyla of bacteria, produces a dense network of EPSs (Figure 11a,b), which provide physical and chemical protection to the microbial community. As demonstrated by several studies, the EPS represents an important substrate for the precipitation of various minerals due to its capacity to bind cations, such as Si, Al, Ca, Mg, and Fe. This is due to the presence of specific functional groups (e.g., carboxylic acids) that have a negatively charged surface (e.g., [15,16,24,75]). The accumulation of ions in the EPS matrix provides enough elements for the precipitation of amorphous nanoparticles, which have been considered to represent the precursors for clay mineral nucleation and growth [22,32,76,77]. The resolution of our data did not allow the detection of the particles at the nano level, but the multi-elemental Si-rich particles observed in the Bagno dell'Acqua system, as well as in the experimental results, may be considered as products derived from the amorphous nanoparticles that act as nucleation sites for Mg-clay and carbonate minerals. Specifically, the production of EPS by microbes belonging to phylum Firmicutes (*Bacillus* sp.), with the high pH values of the water lake (about 9), also increased due to the possible photosynthetic activity of the microbial community, constitutes the site for inducing nucleation and mineral growth of Mg-smectite. The association between Mg-clay and carbonate minerals was already described in the literature (e.g., [17,31,32]), where a detailed sequence leading to the carbonate precipitation is reported. Our study confirms the scheme proposed by [31] for the formation of the calcite fraction of the microbialites (Table 1). In detail, the initial microenvironmental

conditions are influenced by locale pH increases promoted by photosynthetic activity. This inhibits the precipitation of  $\text{CaCO}_3$  because  $\text{Ca}^{2+}$  is preferentially bounded in the EPS [31]. The elevated pH values also trigger diatom dissolution as testified by visible signs of degradation on diatom frustules (Figure 11c and Figure S2), which occurred within the microbial community. Ref. [27] have experimentally shown that diatom communities contribute to the precipitation of Mg-smectite and carbonate minerals in alkaline lakes; thus, the biogenic  $\text{SiO}_2$  could be considered the primary source of silica in the Bagno dell'Acqua microbialites. At this stage, the microenvironment results in being enriched in  $\text{SiO}_2$  and  $\text{Mg}^{2+}$ , favoring Mg-smectite precipitation. Authigenesis of Mg-smectite continues through time and determines the thickening of the microbialites. The newly formed reactive surface (EPS) is broken down by heterotrophic degradation with the consequent release of  $\text{Ca}^{2+}$  cations. This produces a significant increase in the calcium concentration in the microenvironment where the  $\text{Mg}^{2+}$  concentration was significantly lowered, as  $\text{Mg}^{2+}$  cations were confined in the Mg-clay. The increase in the local calcium activity in an almost Mg-free environment promotes the nucleation of calcite around the clay surface (Figure 11c,d). It might represent the small amount of calcite occurring in the microbialites, where the predominance of aragonite is due to the high Mg/Ca ratios typical of the Bagno dell'Acqua water lake (Table 2, [50]). In general, the role of the degradation of organic matter in contributing to the formation of local physico-chemical conditions where the carbonate and calcium contents are supersaturated within the microbial mat, driving carbonate mineral precipitation, has been widely documented [17,19,78,79]. This statement confirms that Mg-clay minerals represent an ideal substrate for the nucleation of carbonate minerals [20,22,23,31,35,72].

The role of photosynthetic bacteria in promoting the authigenesis of Mg-clay minerals was already reproduced in controlled laboratory experiments [80,81], whereas our study provides the evidence of a direct role of Firmicutes (*Bacillus* sp.), isolated from natural microbialites, in Mg-smectite precipitation onto solid media containing Bagno dell'Acqua lake water (as proposed in the conceptual model of Figure 12).

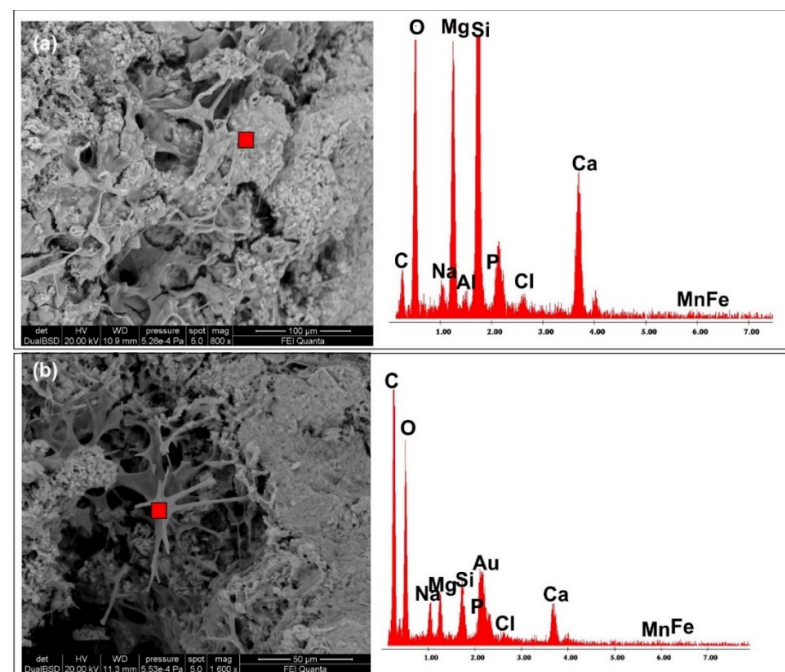
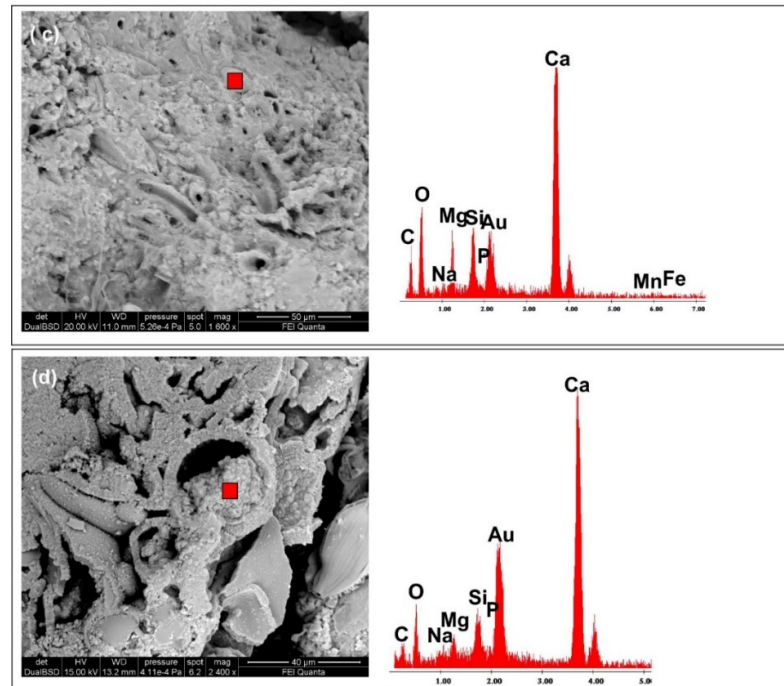
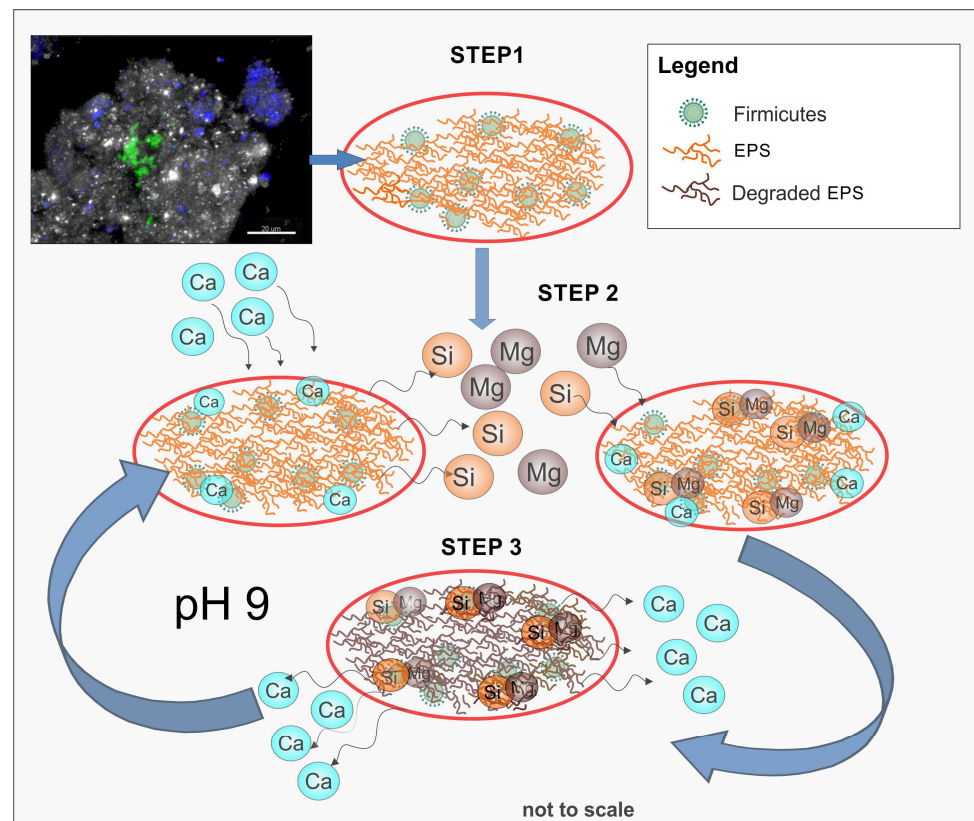


Figure 11. Cont.



**Figure 11.** (a–d) Scanning electron microscopy (SEM) images and relative energy-dispersive X-ray spectra (EDS) showing the association of multi-elemental silicates, Mg-smectite, and carbonate phases with microbes and the extracellular polymeric substance (EPS).



**Figure 12.** Conceptual model (modified after [31]), showing the different stages for the formation of the Bagnò dell'Acqua microbialites: STEP 1—microbial community producing a dense EPS network; STEP 2—suitable condition for nucleation of Mg-smectites and carbonate; STEP 3—heterotrophic degradation of the EPS with the consequent increase in carbonate and calcium content driving carbonate mineral precipitation.



Considering that the interest of the scientific community in understanding the interactions between microorganisms and clay mineral precipitation has been strongly increasing in recent years, the results shown in this study update the list of the natural sites where the association “EPS versus clay-minerals formation” finds suitable conditions for mineral authigenesis, as already observed in other saline and alkaline aquatic environments (e.g., [77,82,83]).

## 5. Conclusions

Until now, reports of the direct role of the microbial community in the precipitation of minerals were attempted under laboratory conditions. This study provides the first evidence of the direct role of the microbes belonging to phylum Firmicutes (*Bacillus* sp.) in promoting the neoformation of Mg-smectite in alkaline waters. This evidence is proven by laboratory experiments, which show that, besides detrital phases, the Bagno dell’Acqua microbialites include significant amounts of various Ca-carbonate and smectite minerals. Scanning electron microscopy energy-dispersive X-ray spectroscopy (SEM-EDS) investigations pointed out the intimate association of Mg-smectite and carbonate minerals with microbes and the extracellular polymeric substance (EPS).

The precipitation of mineral aggregates including Mg-smectite and Ca-carbonate trapped within the EPS has been experimentally driven by culture of *Bacillus* sp. using the Bagno dell’Acqua water lake. In the microbialites of the Bagno dell’Acqua Lake, the sequential mineral precipitation is ruled by the following steps: (1) the microbial community produces a dense EPS network that together with specific physico-chemical conditions provide a suitable substrate for the nucleation of Mg-smectite and carbonate minerals; (2) dissolution of diatom frustules due to the elevated pH leads to a local enrichment in SiO<sub>2</sub> and Mg<sup>2+</sup>; (3) favoring Mg-smectite precipitation; and (4) degradation of the EPS and organic matter leads to the release of Ca<sup>2+</sup> cations with consequent carbonate mineral precipitation.

Finally, the obtained results provide a better understanding of the natural conditions suitable for the development of Mg-smectite microbialites and these findings raised the importance of future research into the wide mechanisms of Mg-clay organo-mineralization.

**Supplementary Materials:** The following supporting information can be downloaded at: <https://www.mdpi.com/article/10.3390/min14101013/s1>, Figure S1: scanning electron microscopy (SEM) images showing (a) centric (sample C4) and (b) pennate diatoms found in the microbialites of the Bagno dell’Acqua lake (sample C10); Figure S2: scanning electron microscopy (SEM) images showing dissolution process acting on diatom frustules (examples from samples C10 and C13); Figure S3: (a) SEM images and (b) EDS spectrum of the laboratory experiment using the Bagno dell’Acqua water lake in the absence of any organism of the microbial community. The experiment was performed at the same operating conditions as the experiment with *Bacillus* sp. 3bis8 strain. EDS spectrum (b) indicate the precipitation of the sole halite aggregates; Figure S4: SEM images and EDS spectrum of the aggregates precipitated by *Escherichia coli* in laboratory experiment using the Bagno dell’Acqua water lake in the same operating conditions as the experiment with *Bacillus* sp. 3bis8 strain. (a,b) The image shows the precipitation of particles composed by prevalent Ca and subordinate Si, Mg and Al elements. Halite is also present as evidenced by EDS spectrum (b). (c,d) SEM image and EDS spectrum of halite aggregates; Table S1: list of microbialites samples recovered along the Bagno dell’Acqua lake with an indication of the type of analysis carried out (SEM-EDS and XRD).

**Author Contributions:** M.I. and F.L.C. conceived and designed the study. M.I. wrote the manuscript with inputs from all coauthors. A.M.C., L.D.B., M.I., F.G.F., F.G. and M.D.B. collected the samples. M.I., A.M.C., L.D.B., C.P. and T.R. prepared the samples and performed the SEM-EDS analyses. A.M.C., C.P., L.A., and T.R. made the classification and geochemistry of the samples. C.M., S.F., A.P., B.C. and A.B. performed the bacterial isolation and identification. L.A. performed XRD analyses. F.G. and M.D.B. made the water geochemical analyses. All authors participated in the writing of the present versions of the manuscript. M.I., F.G.F. and L.A. prepared the figures. All authors have read and agreed to the published version of the manuscript.

**Funding:** This research was financially supported by the project “Conservazione della biodiversità del Lago Bagno dell’Acqua (Isola di Pantelleria)” Prot. N. 0000645 of the 01/03/2022, funded by the Pantelleria National Park and the Sapienza departmental projects 2023 RD12318A998C70B8.

**Data Availability Statement:** Data are contained within the article and Supplementary Materials.

**Acknowledgments:** The authors wish to thank Pantelleria National Park Authority for funding this research and for the logistic support provided. The authors also thank the Advanced Centre for Microscopy “P. Albertano” of University of Rome “Tor Vergata” for CLSM analyses. We would also acknowledge the anonymous reviewers and the Editor for their valuable comments and suggestions that greatly improved the quality of the manuscript.

**Conflicts of Interest:** The authors declare no conflicts of interest.

## References

1. Burne, R.V.; Moore, L.S. Microbialites: Organosedimentary Deposits of Benthic Microbial Communities. *Palaios* **1987**, *2*, 241. [\[CrossRef\]](#)
2. Foster, J.S.; Green, S.J. Microbial diversity in modern stromatolites. In *STROMATOLITES: Interaction of Microbes with Sediments. Cellular Origin, Life in Extreme Habitats and Astrobiology*; Tewari, V., Seckbach, J., Eds.; Springer: Dordrecht, The Netherlands, 2011; Volume 18, pp. 383–405.
3. Reid, R.P.; Macintyre, I.G.; Browne, K.M.; Steneck, R.S.; Miller, T. Modern marine stromatolites in the Exuma Cays, Bahamas: Uncommonly common. *Facies* **1995**, *33*, 1–17. [\[CrossRef\]](#)
4. Chagas, A.A.; Webb, G.E.; Burne, R.V.; Southam, G. Modern lacustrine microbialites: Towards a synthesis of aqueous and carbonate geochemistry and mineralogy. *Earth-Sci. Rev.* **2016**, *162*, 338–363. [\[CrossRef\]](#)
5. Rishworth, G.M.; Dodd, C.; Perissinotto, R.; Bornman, T.G.; Adams, J.B.; Anderson, C.R.; Cawthra, H.C.; Dorrington, R.A.; du Toit, H.; Edworthy, C.; et al. Modern supratidal microbialites fed by groundwater: Functional drivers, value and trajectories. *Earth-Sci. Rev.* **2020**, *210*, 103364. [\[CrossRef\]](#)
6. Suarez-Gonzalez, P.; Benito, M.; Quijada, I.; Mas, R.; Campos-Soto, S. ‘Trapping and binding’: A review of the factors controlling the development of fossil agglutinated microbialites and their distribution in space and time. *Earth-Sci. Rev.* **2019**, *194*, 182–215. [\[CrossRef\]](#)
7. Hoffmann, T.D.; Reeksting, B.J.; Gebhard, S. Bacteria-induced mineral precipitation: A mechanistic review. *Microbiology* **2021**, *167*, 001049. [\[CrossRef\]](#)
8. Braissant, O.; Decho, A.W.; Przekop, K.M.; Gallagher, K.L.; Glunk, C.; Dupraz, C.; Visscher, P.T. Characteristics and turnover of exopolymeric substances in a hypersaline microbial mat. *FEMS Microbiol. Ecol.* **2009**, *67*, 293–307. [\[CrossRef\]](#)
9. Dupraz, C.; Visscher, P.T. Microbial lithification in marine stromatolites and hypersaline mats. *Trends Microbiol.* **2005**, *13*, 429–438. [\[CrossRef\]](#)
10. Reid, R.P.; Visscher, P.T.; Decho, A.W.; Stolz, J.F.; Bebout, B.M.; Dupraz, C.; Macintyre, I.G.; Paerl, H.W.; Pinckney, J.L.; Prufert-Bebout, L.; et al. The role of microbes in accretion, lamination and early lithification of modern marine stromatolites. *Nature* **2000**, *406*, 989–992. [\[CrossRef\]](#)
11. Visscher, P.T.; Stolz, J.F. Microbial mats as bioreactors: Populations, processes, and products. *Palaeogeogr. Palaeoclim. Palaeoecol.* **2005**, *219*, 87–100. [\[CrossRef\]](#)
12. Dupraz, C.; Reid, R.P.; Braissant, O.; Decho, A.W.; Norman, R.S.; Visscher, P.T. Processes of carbonate precipitation in modern microbial mats. *Earth-Sci. Rev.* **2009**, *96*, 141–162. [\[CrossRef\]](#)
13. Visscher, P.T.; Reid, R.P.; Bebout, B.M.; Hoefft, S.E.; Macintyre, I.G.; Thompson, J.A. Formation of lithified micritic laminae in modern marine stromatolites (Bahamas); the role of sulfur cycling. *Am. Mineral.* **1998**, *83 Pt 2*, 1482–1493. [\[CrossRef\]](#)
14. Visscher, P.T.; Reid, R.P.; Bebout, B.M. Microscale observations of sulfate reduction: Correlation of microbial activity with lithified micritic laminae in modern marine stromatolites. *Geology* **2000**, *28*, 919–922. [\[CrossRef\]](#)
15. Dupraz, C.; Visscher, P.T.; Baumgartner, L.K.; Reid, R.P. Microbe–mineral interactions: Early carbonate precipitation in a hypersaline lake (Eleuthera Island, Bahamas). *Sedimentology* **2004**, *51*, 745–765. [\[CrossRef\]](#)
16. Braissant, O.; Decho, A.W.; Dupraz, C.; Glunk, C.; Przekop, K.M.; Visscher, P.T. Exopolymeric substances of sulfate-reducing bacteria: Interactions with calcium at alkaline pH and implication for formation of carbonate minerals. *Geobiology* **2007**, *5*, 401–411. [\[CrossRef\]](#)
17. Pace, A.; Bourillot, R.; Bouton, A.; Vennin, E.; Braissant, O.; Dupraz, C.; Duteil, T.; Bundeleva, I.; Patrier, P.; Galaup, S.; et al. Formation of stromatolite lamina at the interface of oxygenic–anoxygenic photosynthesis. *Geobiology* **2018**, *16*, 378–398. [\[CrossRef\]](#)
18. Cabestrero, Ó.; Sanz-Montero, M.E. Brine evolution in two inland evaporative environments: Influence of microbial mats in mineral precipitation. *J. Paleolimnol.* **2018**, *59*, 139–157. [\[CrossRef\]](#)
19. Sanz-Montero, M.E.; Cabestrero, Ó.; Sánchez-Román, M. Microbial Mg-rich Carbonates in an Extreme Alkaline Lake (Las Eras, Central Spain). *Front. Microbiol.* **2019**, *10*, 148. [\[CrossRef\]](#)
20. Souza-Egipsy, V.; Wierzbos, J.; Ascaso, C.; Neelson, K.H. Mg–silica precipitation in fossilization mechanisms of sand tufa endolithic microbial community, Mono Lake (California). *Chem. Geol.* **2005**, *217*, 77–87. [\[CrossRef\]](#)

21. Bontognali, T.R.; Martinez-Ruiz, F.; McKenzie, J.A.; Bahniuk, A.; Anjos, S.; Vasconcelos, C. Smectite synthesis at low temperature and neutral pH in the presence of succinic acid. *Appl. Clay Sci.* **2014**, *101*, 553–557. [[CrossRef](#)]
22. Burne, R.V.; Moore, L.S.; Christy, A.G.; Troitzsch, U.; King, P.L.; Carnerup, A.M.; Hamilton, P.J. Stevensite in the modern thrombolites of Lake Clifton, Western Australia: A missing link in microbialite mineralization? *Geology* **2014**, *42*, 575–578. [[CrossRef](#)]
23. Pace, A.; Bourillot, R.; Bouton, A.; Vennin, E.; Galaup, S.; Bundeleva, I.; Patrier, P.; Dupraz, C.; Thomazo, C.; Sansjofre, P.; et al. Microbial and diagenetic steps leading to the mineralisation of Great Salt Lake microbialites. *Sci. Rep.* **2016**, *6*, 31495. [[CrossRef](#)] [[PubMed](#)]
24. Perri, E.; Tucker, M.E.; Słowakiewicz, M.; Whitaker, F.; Bowen, L.; Perrotta, I.D. Carbonate and silicate biomineralization in a hypersaline microbial mat (Mesaieed sabkha, Qatar): Roles of bacteria, extracellular polymeric substances and viruses. *Sedimentology* **2018**, *65*, 1213–1245. [[CrossRef](#)]
25. del Buey, P.; Cabestrero, Ó.; Arroyo, X.; Sanz-Montero, M.E. Microbially induced palygorskite-sepiolite authigenesis in modern hypersaline lakes (Central Spain). *Appl. Clay Sci.* **2018**, *160*, 9–21. [[CrossRef](#)]
26. Cuadros, J. Clay minerals interaction with microorganisms: A review. *Clay Miner.* **2017**, *52*, 235–261. [[CrossRef](#)]
27. del Buey, P.; Sanz-Montero, M.; Sánchez-Román, M. Bioinduced precipitation of smectites and carbonates in photosynthetic diatom-rich microbial mats: Effect of culture medium. *Appl. Clay Sci.* **2023**, *238*, 106932. [[CrossRef](#)]
28. Mueller, B. Experimental Interactions Between Clay Minerals and Bacteria: A Review. *Pedosphere* **2015**, *25*, 799–810. [[CrossRef](#)]
29. Tazaki, K. Microbial Formation of a Halloysite-Like Mineral. *Clays Clay Miner.* **2005**, *53*, 224–233. [[CrossRef](#)]
30. Cuadros, J.; Afsin, B.; Jadubansa, P.; Ardakani, M.; Ascaso, C.; Wierzbos, J. Pathways of volcanic glass alteration in laboratory experiments through inorganic and microbially-mediated processes. *Clay Miner.* **2013**, *48*, 423–445. [[CrossRef](#)]
31. Suosaari, E.P.; Lasco, I.; Oehlert, A.M.; Parlanti, P.; Mugnaioli, E.; Gemmi, M.; Machabee, P.F.; Piggot, A.M.; Palma, A.T.; Reid, R.P. Authigenic clays as precursors to carbonate precipitation in saline lakes of Salar de Llamara, Northern Chile. *Commun. Earth Environ.* **2022**, *3*, 325. [[CrossRef](#)]
32. Mather, C.C.; Lampinen, H.M.; Tucker, M.; Leopold, M.; Dogramaci, S.; Raven, M.; Gilkes, R.J. Microbial influence on dolomite and authigenic clay mineralisation in dolomite profiles of NW Australia. *Geobiology* **2023**, *21*, 644–670. [[CrossRef](#)]
33. McCutcheon, J.; Power, I.M.; Shuster, J.; Harrison, A.L.; Dipple, G.M.; Southam, G. Carbon Sequestration in Biogenic Magnesium and Other Magnesium Carbonate Minerals. *Environ. Sci. Technol.* **2019**, *53*, 3225–3237. [[CrossRef](#)] [[PubMed](#)]
34. Zhou, C.H.; Keeling, J. Fundamental and applied research on clay minerals: From climate and environment to nanotechnology. *Appl. Clay Sci.* **2013**, *74*, 3–9. [[CrossRef](#)]
35. Bischoff, K.; Sirantoine, E.; Wilson, M.E.J.; George, A.D.; Monteiro, J.M.; Saunders, M. Spherulitic microbialites from modern hypersaline lakes, Rottneest Island, Western Australia. *Geobiology* **2020**, *18*, 725–741. [[CrossRef](#)] [[PubMed](#)]
36. Zeyen, N.; Benzerara, K.; Li, J.; Groleau, A.; Balan, E.; Robert, J.-L.; Estève, I.; Tavera, R.; Moreira, D.; López-García, P. Formation of low-T hydrated silicates in modern microbialites from Mexico and implications for microbial fossilization. *Front. Earth Sci.* **2015**, 1–23. [[CrossRef](#)]
37. Zeyen, N.; Benzerara, K.; Beyssac, O.; Daval, D.; Muller, E.; Thomazo, C.; Tavera, R.; López-García, P.; Moreira, D.; Duprat, E. Integrative analysis of the mineralogical and chemical composition of modern microbialites from ten Mexican lakes: What do we learn about their formation? *Geochim. Cosmochim. Acta* **2021**, *305*, 148–184. [[CrossRef](#)]
38. Kazmierczak, J.; Kempe, S.; Kremer, B.; López-García, P.; Moreira, D.; Tavera, R. Hydrochemistry and microbialites of the alkaline crater lake Alchichica, Mexico. *Facies* **2011**, *57*, 543–570. [[CrossRef](#)]
39. Arp, G.; Reimer, A.; Reitner, J. Microbialite Formation in Seawater of Increased Alkalinity, Satonda Crater Lake, Indonesia. *J. Sediment. Res.* **2003**, *73*, 105–127. [[CrossRef](#)]
40. Arp, G.; Reimer, A.; Reitner, J. Microbialite Formation in Seawater of Increased Alkalinity, Satonda Crater Lake, Indonesia: Reply. *J. Sediment. Res.* **2004**, *74*, 318–325. [[CrossRef](#)]
41. Kazmierczak, J.; Kempe, S. Modern terrestrial analogues for the carbonate globules in Martian meteorite ALH84001. *Sci. Nat.* **2003**, *90*, 167–172. [[CrossRef](#)]
42. DiLoreto, Z.A.; Bontognali, T.R.R.; Al Disi, Z.A.; Al-Kuwari, H.A.S.; Williford, K.H.; Strohmenger, C.J.; Sadooni, F.; Palermo, C.; Rivers, J.M.; McKenzie, J.A.; et al. Microbial community composition and dolomite formation in the hypersaline microbial mats of the Khor Al-Adaid sabkhas, Qatar. *Extremophiles* **2019**, *23*, 201–218. [[CrossRef](#)] [[PubMed](#)]
43. Bontognali, T.R.R.; Vasconcelos, C.; Warthmann, R.J.; Bernasconi, S.M.; Dupraz, C.; Strohmenger, C.J.; McKenzie, J.A. Dolomite formation within microbial mats in the coastal sabkha of Abu Dhabi (United Arab Emirates). *Sedimentology* **2010**, *57*, 824–844. [[CrossRef](#)]
44. D’Alessandro, W.; Dongarrà, G.; Gurrieri, S.; Parello, F.; Valenza, M. Geochemical characterization of naturally occurring fluids on the Island of Pantelleria (Italy). *Mineral. Petrogr. Acta* **1994**, *37*, 91–102.
45. Parello, F.; Allard, P.; D’Alessandro, W.; Federico, C.; Jean-Baptiste, P.; Catani, O. Isotope geochemistry of Pantelleria volcanic fluids, Sicily Channel rift: A mantle volatile end-member for volcanism in southern Europe. *Earth Planet. Sci. Lett.* **2000**, *180*, 325–339. [[CrossRef](#)]
46. Aiuppa, A.; D’Alessandro, W.; Gurrieri, S.; Madonna, P.; Parello, F. Hydrologic and geochemical survey of the lake “Specchio di Venere” (Pantelleria island, Southern Italy). *Environ. Geol.* **2007**, *53*, 903–913. [[CrossRef](#)]

47. Pecoraino, G.; D'Alessandro, W.; Inguaggiato, S. *The Other Side of the Coin: Geochemistry of Alkaline Lakes in Volcanic Areas*; Springer: Berlin/Heidelberg, Germany, 2015; pp. 219–237.
48. Cangemi, M.; Madonna, P.; Speziale, S. Geochemistry and mineralogy of a complex sedimentary deposit in the alkaline volcanic Lake Specchio di Venere (Pantelleria Island, south Mediterranean). *J. Limnol.* **2018**, *77*, 220–231. [[CrossRef](#)]
49. Cangemi, M.; Bellanca, A.; Borin, S.; Hopkinson, L.; Mapelli, F.; Neri, R. The genesis of actively growing siliceous stromatolites: Evidence from Lake Specchio di Venere, Pantelleria Island, Italy. *Chem. Geol.* **2010**, *276*, 318–330. [[CrossRef](#)]
50. Cangemi, M.; Censi, P.; Reimer, A.; D'Alessandro, W.; Hause-Reitner, D.; Madonna, P.; Oliveri, Y.; Pecoraino, G.; Reitner, J. Carbonate precipitation in the alkaline lake Specchio di Venere (Pantelleria Island, Italy) and the possible role of microbial mats. *Appl. Geochem.* **2016**, *67*, 168–176. [[CrossRef](#)]
51. Bruschini, E.; Ferrari, M.; Mazzoni, C.; Fazi, S.; Chiocci, F.L.; Mazzini, I.; Costanzo, G.; De Angelis, S.; De Sanctis, M.C.; Altieri, F.; et al. Preliminary spectroscopic investigation of a potential Mars analog site: Lake Bagno dell'Acqua, Pantelleria, Italy. *Planet. Space Sci.* **2024**, *245*, 105893. [[CrossRef](#)]
52. Azzaro, E.; Badalamenti, F.; Dongarrà, G.; Hauser, S. Geochemical and mineralogical studies of Lake Specchio di Venere, Pantelleria Island, Italy. *Chem. Geol.* **1983**, *40*, 149–165. [[CrossRef](#)]
53. Civetta, L.; Cornette, Y.; Gillot, P.Y.; Orsi, G. The eruptive history of Pantelleria (Sicily channel) in the last 50 ka. *Bull. Volcanol.* **1988**, *50*, 47–57. [[CrossRef](#)]
54. Civetta, L.; Cornette, Y.; Crisci, G.; Gillot, P.Y.; Orsi, G.; Requejo, C.S. Geology, geochronology and chemical evolution of the island of Pantelleria. *Geol. Mag.* **1984**, *121*, 541–562. [[CrossRef](#)]
55. Censi, P.; Cangemi, M.; Brusca, L.; Madonna, P.; Saiano, F.; Zuddas, P. The behavior of rare-earth elements, Zr and Hf during biologically-mediated deposition of silica-stromatolites and carbonate-rich microbial mats. *Gondwana Res.* **2015**, *27*, 209–215. [[CrossRef](#)]
56. Moore, D.M.; Reynolds, R.C., Jr. *X-ray Diffraction and the Identification and Analysis of Clay Minerals*; Oxford University Press: Oxford, UK, 1997; 378p.
57. Marvasi, M.; Gallagher, K.L.; Martinez, L.C.; Pagan, W.C.M.; Santiago, R.E.R.; Vega, G.C.; Visscher, P.T. Importance of B4 Medium in Determining Organomineralization Potential of Bacterial Environmental Isolates. *Geomicrobiol. J.* **2012**, *29*, 916–924. [[CrossRef](#)]
58. Mazzoni, C.; Piacentini, A.; Di Bella, L.; Aldega, L.; Perinelli, C.; Conte, A.M.; Ingrassia, M.; Ruspandini, T.; Bonfanti, A.; Caraba, B.; et al. Carbonate precipitation and phosphate trapping by microbialite isolates from an alkaline insular lake (Bagno dell'Acqua, Pantelleria Island, Italy). *Front. Microbiol.* **2024**, *15*, 1391968. [[CrossRef](#)] [[PubMed](#)] [[PubMed Central](#)]
59. Tomassetti, M.C.; Cirigliano, A.; Arrighi, C.; Negri, R.; Mura, F.; Maneschi, M.L.; Gentili, M.D.; Stirpe, M.; Mazzoni, C.; Rinaldi, T. A role for microbial selection in frescoes' deterioration in Tomba degli Scudi in Tarquinia, Italy. *Sci. Rep.* **2017**, *7*, 6027. [[CrossRef](#)]
60. Ventura, M.; Casas, I.A.; Morelli, L.; Callegari, M.L. Rapid Amplified Ribosomal DNA Restriction Analysis (ARDRA) Identification of *Lactobacillus* spp. Isolated from Fecal and Vaginal Samples. *Syst. Appl. Microbiol.* **2000**, *23*, 504–509. [[CrossRef](#)]
61. Lupini, G.; Proia, L.; Di Maio, M.; Amalfitano, S.; Fazi, S. CARD-FISH and confocal laser scanner microscopy to assess successional changes of the bacterial community in freshwater biofilms. *J. Microbiol. Methods* **2011**, *86*, 248–251. [[CrossRef](#)]
62. Fazi, S.; Amalfitano, S.; Venturi, S.; Pacini, N.; Vazquez, E.; Olaka, L.A.; Tassi, F.; Crognale, S.; Herzsprung, P.; Lechtenfeld, O.J.; et al. High concentrations of dissolved biogenic methane associated with cyanobacterial blooms in East African lake surface water. *Commun. Biol.* **2021**, *4*, 1–12. [[CrossRef](#)]
63. Meier, H.; Amann, R.; Ludwig, W.; Schleifer, K.H. Specific Oligonucleotide Probes for in situ Detection of a Major Group of Gram-positive Bacteria with low DNA G+C Content. *Syst. Appl. Microbiol.* **1999**, *22*, 186–196. [[CrossRef](#)]
64. Fazi, S.; Amalfitano, S.; Piccini, C.; Zoppini, A.; Puddu, A.; Pernthaler, J. Colonization of overlaying water by bacteria from dry river sediments. *Environ. Microbiol.* **2008**, *10*, 2760–2772. [[CrossRef](#)]
65. Venturi, S.; Crognale, S.; Di Benedetto, F.; Montegrossi, G.; Casentini, B.; Amalfitano, S.; Baroni, T.; Rossetti, S.; Tassi, F.; Capecchiacci, F.; et al. Interplay between abiotic and microbial biofilm-mediated processes for travertine formation: Insights from a thermal spring (Piscine Carletti, Viterbo, Italy). *Geobiology* **2022**, *20*, 837–856. [[CrossRef](#)] [[PubMed](#)]
66. Chamley, H. *Clay Sedimentology*; Springer: Berlin/Heidelberg, Germany, 1989; p. 623.
67. Parkhurst, D.L.; Appelo, C.A.J. *Description of Input and Examples for PHREEQC Version 3—A Computer Program for Speciation, Batch-Reaction, One-Dimensional Transport, and Inverse Geochemical Calculations*; U.S. Geological Survey Techniques and Methods, 2013; Hydrochemical Consultant Valeriusstraat 11 1071 MB Amsterdam, NL; Book 6, Chapter A43; 497p. Available online: <http://pubs.usgs.gov/tm/06/a43/> (accessed on 6 November 2023).
68. Wright, V.P. Lacustrine carbonates in rift settings: The interaction of volcanic and microbial processes on carbonate deposition. *Geol. Soc. Lond. Spec. Publ.* **2012**, *370*, 39–47. [[CrossRef](#)]
69. Di Figlia, M.G.; Bellanca, A.; Neri, R.; Stefansson, A. Chemical weathering of volcanic rocks at the island of Pantelleria, Italy: Information from soil profile and soil solution investigations. *Chem. Geol.* **2007**, *246*, 1–18. [[CrossRef](#)]
70. Jones, B.F.; Mumpton, F.A. Clay mineral diagenesis in lacustrine sediments. *US Geol. Surv. Bull.* **1986**, *1578*, 291–300.
71. Deocampo, D.M. Evaporative evolution of surface waters and the role of aqueous CO<sub>2</sub> in magnesium silicate precipitation: Lake Eyasi and Ngorongoro crater, northern Tanzania. *S. Afr. J. Geol.* **2005**, *108*, 493–504. [[CrossRef](#)]
72. Tosca, N.J.; Wright, V.P. The formation and diagenesis of Mg-clay minerals in lacustrine carbonate reservoirs. In Proceedings of the 2014 AAPG Annual Convention and Exhibition, Houston, TX, USA, 6–9 April 2014.

73. Lamérand, C.; Shirokova, L.S.; Bénézeth, P.; Rols, J.L.; Pokrovsky, O.S. Olivine dissolution and hydrous Mg carbonate and silicate precipitation in the presence of microbial consortium of photo-autotrophic and heterotrophic bacteria. *Geochim. Cosmochim. Acta* **2020**, *268*, 123–141. [[CrossRef](#)]
74. Duchi, V.; Campana, M.E.; Minissale, A.; Thompson, M. Geochemistry of thermal fluids on the volcanic isle of Pantelleria, southern Italy. *Appl. Geochem.* **1994**, *9*, 147–160. [[CrossRef](#)]
75. Moore, K.R.; Pajusalu, M.; Gong, J.; Sojo, V.; Matreux, T.; Braun, D.; Bosak, T. Biologically mediated silicification of marine cyanobacteria and implications for the Proterozoic fossil record. *Geology* **2020**, *48*, 862–866. [[CrossRef](#)]
76. Perri, E.; Manzo, E.; Tucker, M.E. Multi-scale study of the role of the biofilm in the formation of minerals and fabrics in calcareous tufa. *Sediment. Geol.* **2012**, *263–264*, 16–29. [[CrossRef](#)]
77. Perri, E.; Słowakiewicz, M.; Perrotta, I.D.; Tucker, M.E. Biomineralization processes in modern calcareous tufa: Possible roles of viruses, vesicles and extracellular polymeric substances (Corvino Valley–Southern Italy). *Sedimentology* **2022**, *69*, 399–422. [[CrossRef](#)]
78. López-García, P.; Kazmierczak, J.; Benzerara, K.; Kempe, S.; Guyot, F.; Moreira, D. Bacterial diversity and carbonate precipitation in the giant microbialites from the highly alkaline Lake Van, Turkey. *Extremophiles* **2005**, *9*, 263–274. [[CrossRef](#)] [[PubMed](#)]
79. Decho, A.W. Microbial biofilms in intertidal systems: An overview. *Cont. Shelf Res.* **2000**, *20*, 1257–1273. [[CrossRef](#)]
80. Lamérand, C.; Shirokova, L.S.; Bénézeth, P.; Rols, J.-L.; Pokrovsky, O.S. Carbon sequestration potential of Mg carbonate and silicate biomineralization in the presence of cyanobacterium *Synechococcus*. *Chem. Geol.* **2022**, *599*, 120854. [[CrossRef](#)]
81. Lamérand, C.; Shirokova, L.S.; Petit, M.; Bénézeth, P.; Rols, J.; Pokrovsky, O.S. Kinetics and mechanisms of cyanobacterially induced precipitation of magnesium silicate. *Geobiology* **2022**, *20*, 560–574. [[CrossRef](#)]
82. Leguey, S.; De León, D.R.; Ruiz, A.I.; Cuevas, J. The role of biomineralization in the origin of sepiolite and dolomite. *Am. J. Sci.* **2010**, *310*, 165–193. [[CrossRef](#)]
83. Leveille, R.J.; Juniper, S.K. Microbial colonization and weathering of sulphide minerals at deep-sea hydrothermal vents: In situ exposure experiments. *Cah. De Biol. Mar.* **2002**, *43*, 285–288.

**Disclaimer/Publisher’s Note:** The statements, opinions and data contained in all publications are solely those of the individual author(s) and contributor(s) and not of MDPI and/or the editor(s). MDPI and/or the editor(s) disclaim responsibility for any injury to people or property resulting from any ideas, methods, instructions or products referred to in the content.